Regional Climate Simulation of the 1998 Summer Flood over East Asia

Dong-Kyou Lee, Dong-Hyun Cha and Hyun-Suk Kang

Atmospheric Sciences Program, School of Earth and Envornmental Sciences
Seoul National University, Seoul 151-742, KOREA

1. Introduction

The regional climate over East Asia is governed not only by large-scale monsoon circulation but also by mesoscale physical processes as well as nonlinear scale-interactions between large- and small-scale environments. During the 1998 summer monsoon period, China, Korea and Japan over East Asia have experienced record-breaking heavy rainfalls. In particular, the 18-day long lasted heavy rainfall events occurring over the Korean peninsula from 31 July to 17 August were characterized by unprecedental statistics, that is, the number of heavy rainfall events was 16 times with a record-breaking daily precipitation amount of 617.5 mm and hourly precipitation intensity of 145.0 mm at Kangwha in the middle part of the peninsula. Heavy rainfall events over southern Korea occurred about 6 times per year from 1980 to 1990 during the summer of June through September (Lee et al., 1998).

In this study, we performed three-month long regional climate simulation of the 1998 summer (June, July and August) using the Seoul National University/Regional Climate Model (SNU/RCM) which is based on the MM5 and the NCAR Land Surface Model, which will be described in more detail in section 2. The objectives of this study are to simulate the evolution of this extreme regional climate over East Asia using the SNU/RCM and to evaluate the performance of model simulation of heavy precipitation events during the 1998 summer.

2. Model Description

The SNU/RCM (Lee and Kang, 1999) has been developed on the basis of the latest release of MM5 version 2 (MM5V2; Grell et al., 1994). The noteworthy modifications of SNU/RCM in comparison with the standard version of MM5 for application to climate simulation are the implementation of an advanced NCAR land surface process (Bonan, 1996), and of a spectral nudging technique (von Storch et al., 2000) including a modified relaxation method. A minor change for taking account for variation of sea surface temperature has been also made.

The model domain consists of 145 and 121 grid points in the zonal and meridional direction (7200 km × 6000 km), respectively, centered at 35°N and 120°E with the horizontal grid spacing of 50 km (Figure 1). In the vertical, there are 31 σ-layers between the 70 hPa top and the surface. The physical processes used in this study are Grell's cumulus parameterization, simple ice cloud microphysics, MRF PBL scheme and CCM2 radiation package. The NCAR land surface model (LSM) is a one-dimensional model of energy, momentum, water exchanges between the atmosphere and land by taking account for (1) ecological differences among vegetation types, (2) thermal and hydrological differences among soil types, and (3) multiple surface types including lakes and wetlands within a grid cell (Bonan, 1996). It also considers sub-grid scale heterogeneity of surface types using mosaic-type combination of multiple plant type functions within a grid cell.

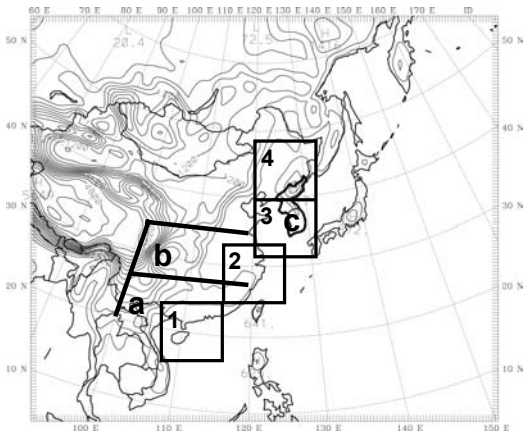

Fig. 1. The model domain and tophograph. The region a, b, c indicate South China (20~27°N), Central China (27~35°N), and Korea peninsula respectively. The square 1, 2, 3, 4 are the hydrology calculated regions.

The spectral nudging technique developed by von Storch et al. (2000) is also used along with the relaxation method in order to reduce systematic biases accompanying with the lateral boundary condition. Differently from the conventional approach, the relaxation method, driving forcings in the spectral nudging technique are not only stipulated at the lateral boundaries but also in the model interior. These are maintained by adding nudging terms to the model equations for horizontal wind and moisture in the spectral domain, with maximum efficiency for large scales and no effect for small scales. There have been previous studies that share similarities in terms of scale separation using spectral method (Kida et al., 1991), but this is a unique approach because model solutions are nudged with large-scale driving fields. In the spectral nudging technique, the buffer zone at the lateral boundaries is still kept and an additional steering is introduced in the model interior for the horizontal wind and moisture fields.

In order to provide initial and boundary data required for deriving the regional climate model, upper-air variables (zonal and meridional winds, temperature, and relative humidity) of 2.5° × 2.5° interval at 13 pressure levels from 1000 to 70 hPa and surface variables of T63 Gaussian grids

(approximately $1.875^{o} \times 1.904^{o}$ interval) are obtained from 6-hourly NCEP/DOE2 reanalysis (Kistler et al., 2001) after bi-linear interpolation to the model grids. Observed sea surface temperature (SST) is used updating every 24 hours from the $1^{o} \times 1^{o}$ weekly data (Reynolds and Smith, 1994). Additional surface boundary conditions required for the NCAR LSM, which are surface types, soil color, soil texture including lake/wetlands fraction. The sources of these data were described in Lee and Kang (1999). The SNU/RCM requires initial soil moisture and temperature fields, which are obtained by integrating the off-line NCAR/LSM repeatedly until the changes of soil water content reaches equilibrium state under the forcing of 6-hourly atmospheric values and surface radiation from NCEP reanalysis as well as observed daily precipitation from NCEP/CPC archives for the year of 1998.

3. Results and Discussion

Time series of area-averaged daily precipitation over southern China, central China, and the Korean peninsula are shown in Figure 2. Station observed precipitation data come from the archives of NCEP Climate Prediction Center (CPC). Not only precipitation amount but also its temporal evolution simulated by the SNU/RCM show agreement with observation except for the region of southern China especially during the last half of June and July, when the simulated precipitation is underestimated less than one-half comparing to the observation. The underestimated precipitation for the last half of June over southern China seems to partially result from northward shift of monsoon rain-belt in the model. In central China the simulated rain is in agreement with observation in June in which severe floodings in central China took place, while there is much underestimated simulated precipitation from mid-July.

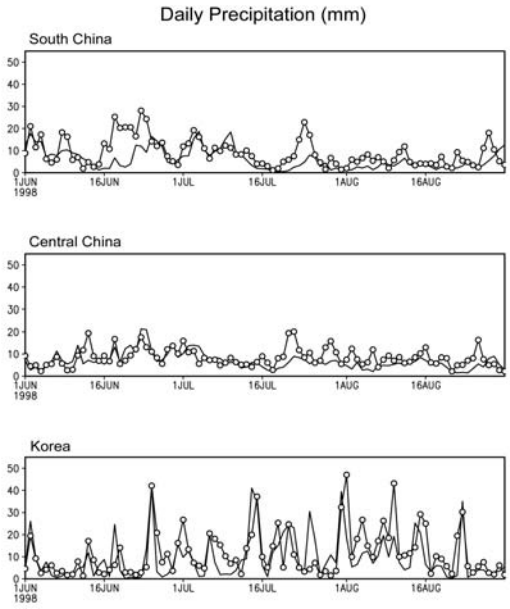

Fig. 2. Time series of area averaged daily precipitation over southern China (upper), central China (middle), and Korean peninsula.

Figure 3 shows the composite chart of monthly averaged large-scale features containing 200hPa wind speed greater than 25 ms^{-1}, vertical integrated moisture transport, and precipitation. The observed precipitation is from CPC Merged Analysis of Precipitation (CMAP) and moisture flux and wind speeds are from NCEP reanalysis. The composite chart describes favorable conditions for heavy precipitation, in which maximum rainfall areas are located south to the upper level jet (ULJ) and north to the low level jet (LLJ). It is clearly shown that the precipitation amount is significantly related with the ULJ intensity in both simulation results and reanalysis. At the upper level, the spatial distribution of simulated wind speed was comparable to reanalysis, but its strength is underestimated slightly about less than 2 ms^{-1} compared to reanalysis.

In June, the simulated monsoon rain is shifted southward over the northwestern Pacific Ocean, while it is shifted northward over central China about 2 degree in latitude compared with the CMAP observation. The horizontal distribution of precipitation in June is simulated reasonably compared to observation, except for coastal region of southern China, where heavy rainfall is observed. These differences between the observed and the simulated precipitation seem to be related with moisture convergence, which will be further investigated later using atmospheric moisture budget analysis. In August, simulated precipitation over Korean peninsula is underestimated significantly compared to the CMAP observation and the maximum rainfall region is located over northern Korea, but the observed maximum region was over central Korea. The reason of this large discrepancy between observed and simulated precipitation is due to the northward shift of moisture transport, especially during the period of the first half of August, when record-breaking heavy rainfalls occurred.

The area-averaged hydrology budgets of model and reanalysis over four sub-regions (see Figure 1) were calculated in order to investigate the discrepancies between observed and simulated precipitation (Figure 4). The hydrology budget can be calculated by $W=E-P+C+R$, where W is the total change of precipitable water, E and P are surface evaporation and precipitation, respectively, C the vertically integrated atmospheric moisture convergence, and R the diffusion of water vapor which is assumed to be a residual term (Bosilovich and Sun, 1999). We calculated atmospheric hydrology budget from monthly averaged model output and reanalysis data. In June, the moisture convergence over region 1 (south coastal area of China) is underestimated significantly compared to reanalysis, which is mainly resulted from the increased northward outflow of moisture. On the contrary, over the region 2 (near the Yangtze River), moisture convergence is overestimated not only by the increased inflow of moisture through western boundary but also decreased outflow of moisture through eastern boundary compared to reanalysis data. Therefore, the simulated precipitation amount over region 1 decreased about 30 % to that of CMAP observation because of the decreased moisture convergence, while precipitation amount over region 2 increased slightly due to the increased moisture convergence. In August, we can see clearly that

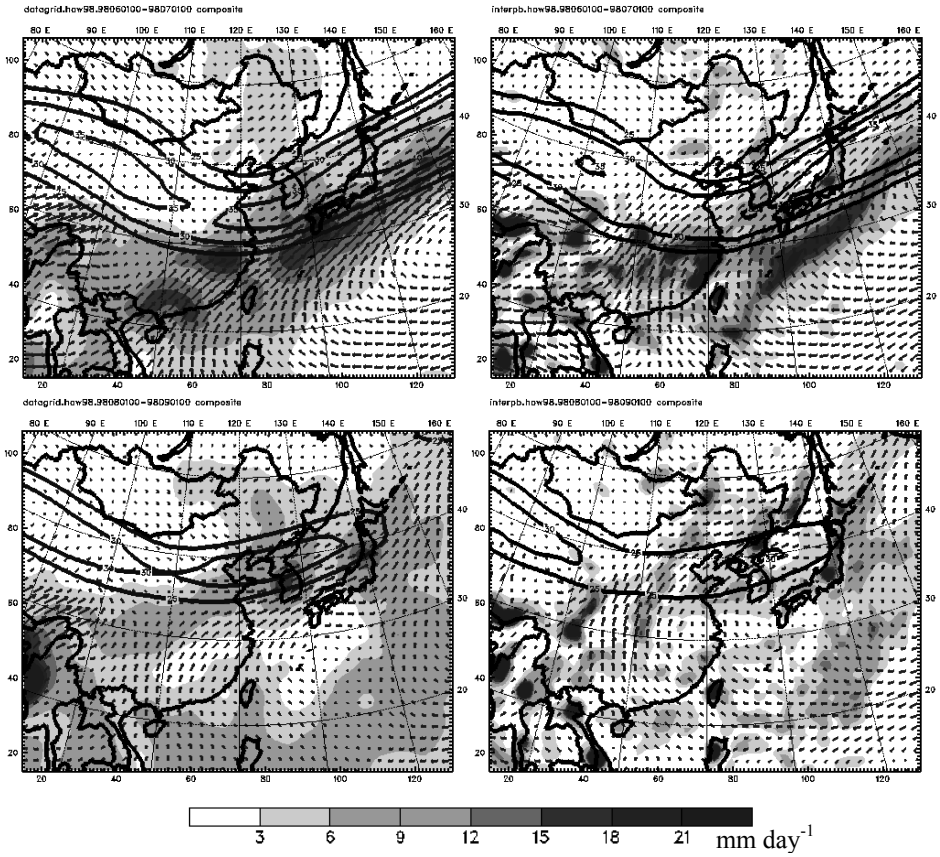

Fig. 3. Monthly mean composite chart of 200 hPa wind speed greater than 25 ms^{-1} (contour), vertically integrated moisture transport (vectors), and precipitation (shaded) for the NCEP/DOE2 reanalysis (left panel) and simulation results (right panel) in June (upper)

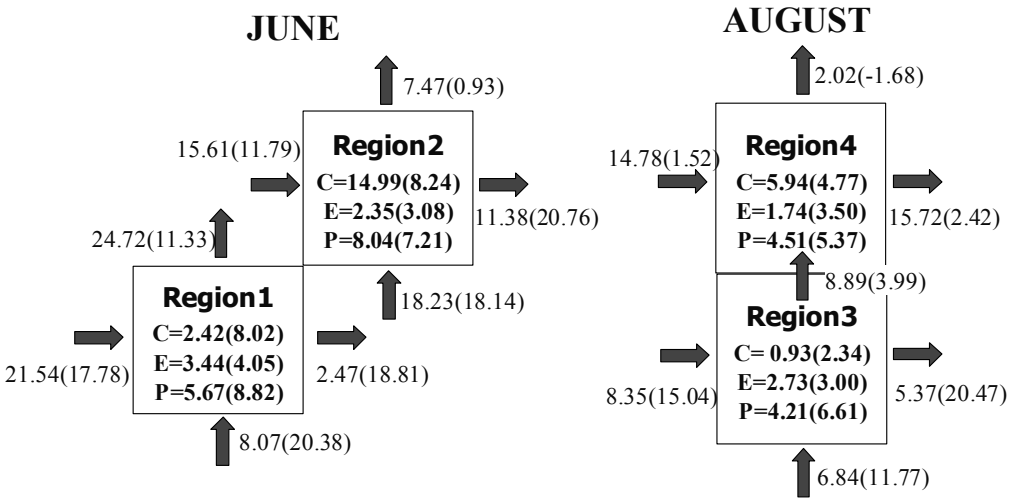

Fig. 4. The hydrology budget over four sub regions. Values in parenthesis are calculated from reanalysis data. The units are mm day^{-1}. Details are described in the text.

Table 1. Monthly mean statistics for 850 hPa mixing ratio, wind speed and sea level pressure.

Month	850 hPa Mixing ratio ($g\ kg^{-1}$)			850 hPa wind speed ($m\ s^{-1}$)			Sea level pressure (hPa)		
	BIAS	RMSE	SC	BIAS	RMSE	SC	BIAS	RMSE	SC
June	1.84	3.61	0.66	0.48	1.70	0.85	1.60	1.83	0.96
July	1.48	3.86	0.37	0.63	1.98	0.86	1.28	1.78	0.90
August	1.42	3.38	0.48	0.66	2.31	0.71	1.32	1.94	0.71

moisture transport flow in zonal direction near the Korean peninsula (regions 3 and 4) is shifted northward compared to reanalysis data. In addition, the moisture transport from region 3 to region 4 in meridional direction increased greater than two times compared to that of reanalysis. These discrepancies of moisture transport between the simulation results and reanalysis data may attribute to brings about underestimated precipitation over region 3 due to the decreased moisture convergence and vice versa over region 4.

In this study, we applied spectral nudging technique to the moisture fields as well as horizontal wind fields. To evaluate the performance of the SNU/RCM, bias, RMSE and spatial correlation coefficient between the simulation results and NCEP/DOE2 reanalysis for the variables of 850 hPa mixing ratio, wind speed and sea level pressure are shown in Table 1. These were calculated over the entire model domain excluding lateral boundary buffer area, which corresponds about 20 grid pointes from each boundary. The biases and correlation coefficients for mixing ratio are found to be relatively poor significantly than those of other fields, while biases and correlation of coefficients at the surface are between ±0.5 g/kg and greater than 0.95, respectively. Spatial patterns of sea level pressure deviates greatly from those of the reanalysis data in August in which correlation coefficients rapidly decrease from 0.90 in July to 0.71 in August. Results of these statistics imply that the spectral nudging for moisture fields contaminates the model solutions during the integration.

4. Summary

The 1998 summer flood, in which record-breaking heavy rainfall events occurred over East Asia, was simulated using the SNU/RCM in order to evaluate the model performance in simulating extreme regional climates. The monthly mean features of atmospheric circulation are simulated comparable to the reanalysis data. Temporal evolution of precipitation also fairy reproduces the observation, except over Southern China. However, there exist considerable discrepancies in horizontal distribution of precipitation between the simulation and observation, especially in August. The underestimation over southern coastal area of China in June results from decreased moisture convergence due to strong northward outflow of moisture in the model. Heavy rainfalls along the monsoon front occurring over Korea during early August are also underestimated and located north to the observation because of the northward outflow of moisture. These differences in moisture fields seem to be resulted from the spectral nudging for moisture fields, which will be further investigated in the future. A high-resolution regional climate simulation using one-way nesting approach for this case is suggested to examine these 18-day consecutive heavy rain events over the Korean peninsula.

Acknowledgements

This study is supported through the BK21 program by the Ministry of Education of Korean government. The authors also appreciate to Ms. Frauker at Max Planck Institute for providing routines of spectral nudging and to NCAR for providing access to the valuable surface observation data.

References

Bonan, G. B., 1996: *A land surface model (LSM version 1.0) for ecological, hydrological, and atmospheric studies: Technical description and user's guide.* NCAR/TN-417+STR, NCAR Technical Note, NCAR, Boulder, CO. 150pp.

Bosilovich M. G., and W.-Y. Sun, 1999: Numerical simulation of the 1993 midwestern flood: Land-atmosphere interaction. *J. Climate*, **12**, 1490-1505.

Grell, G. A., J. Dudhia, and D. R. Stauffer, 1994*: A description of the fifth-generation Penn State/NCAR mesoscale model (MM5)*. NCAR/TN-398+STR, NCAR Technical Note, NCAR, Boulder, CO. 122pp.

Kida, H., T. Koide, H. Sasaki, and M. Chiba, 1991: A new approach to coupling a limited area model with a CGM for regional climate simulation. *J. Meteor. Soc. of Japan*, **69**, 723-728.

Kistler, R. and coathutors, 2001: The NCEP-NCAR 50-year reanalysis: Monthly means CD-ROM and documentation. *Bull. Amer. Meteor. Soc*., **82**, 247-267.

Lee, D.-K., H.-R. Kim, and S.-Y. Hong, 1998: Heavy precipitation over Korea during 1980-1990. *Koean J. Atmos. Sci.*, **1**, 32-50.

Lee, D.-K., and H.-S., Kang, 1999: Coupling of the NCAR/LSM into the MM5 and its application for the East Asian summer monsoon. *Preprints of the ninth PSU/NCAR mesoscale model users' workshop*. 23-25 June 1999, Boulder, CO., 198-201.

Reynolds R. W., and T. M. Smith, 1994: Improved global sea surface temperature analyses. *J. Climate*, **7**, 929-948.

Von Storch, H., H. Langenberg, and F. Feser, 2000: A spectral nudging for dynamical downscaling purposes. *Mon. Wea. Rev.*, **128**, 3664-3673.